SYNTHESIS ZINC OXIDE NANOPARTICLES USING ZINC CHLORIDE, ZINC NITRATE HEXAHYDRATE AND ZINC ACETATE DIHYDRATE PRECURSORS FOR ANTIBACTERIAL APPLICATIONS

A Thesis Submitted to Applied Physics Program Adama Science and Technology University

In Partial Fulfillment of the Requirements for the Degree of Master of Science in Physics

By: Segedie Getie Worku

Advisor: Dr. Abebe Belay Gemta (Associate Professor)

June, 2017

Adama, Ethiopia

APPROVAL SHEET

ADAMA SCIENCE AND TECHNOLOGY UNIVERSITY

SCHOOL OF APPLIED NATURAL SCIENCE

APPLIED PHYSICS PROGRAM

This is to certify that the thesis prepared by **Segedie Getie** entitle **"Synthesis zinc oxide nanoparticles using zinc chloride, zinc nitrate hexahydrate and zinc acetate dihydrate precursors for antibacterial applications"** submitted in fulfillment of the requirement for the degree of master of science in physics complies with the regulation of the university and meets the accepted standards with respect to originality.

Signed by the examination committee

Name	Signature	Date
.....	.....	.....
(Advisor)		
.....	.....	.....
(Chairman)		
.....	.....	.....
(External Examiner)		
.....	.....	.....
(Internal Examiner)		

ACKNOWLEDGEMENTS

First of all, I am gratefully indebted to the almighty God whose everlasting and undying love kept me and for his infinite mercy throughout my life and during the course of this thesis work.

My sincere thanks go to my advisor Dr. Abebe Belay for his patience; understanding and critical concerns made this research work a great success. Also special thanks to Prof. A.RammaChandra Reddy for his interesting advice and support during laboratory work and creating opportunity to send my sample to Indian for XRD characterization.

I acknowledge and appreciate my beloved classmates and friends all those who contributed in one way or the other to the fulfilment of this research work specially Semahegn Asemare and Bulcha Bekele who are closest as two faces of one coin friendship to me and are always with me during laboratory work.

I would like to acknowledge AAU department of chemistry allowing me UV-Vis, fluorescence spectroscopy and IR Instrument, and National Institute of Technology, Materials Science Laboratory, India for allowing XRD characterization of my samples. And also Pusan National University, Department of Nanoscience and Nanotechnology, South Korea for allowing SEM characterization of my samples.

My sincere thanks also go to Dr. K. Sowri Babu and Dr. Ermias Libnedengel Tsigie who characterize the XRD and SEM characterization of my samples respectively.

I have no words to express my thanks to Dr. Zerihun Belay and Mr.Temesgen Assefa who have assisted me the microbial laboratory activity. My unlimited acknowledge goes to oromia public health research capacity building and quality assurance laboratory center (regional lab) for providing me the standard antibiotic drugs.

I would like to express my greatest thanks to Dr. Mesfin Asfaw, head department of physics, for his support, and to Dr. Tewodros Yirgashewa, Dr. Megersa Wedajo and Dr. Alemu Kebede for providing me indispensable knowledge in the corresponding courses.

Finally, my thanks go to my wonderful and caring parents specially my father Getie Worku and my mother Degitu Lakew for their love, moral, and financial support towards my education.

Dedication

This work is dedicated to:

My father: Getie Worku

My mother: Degitu Lakew

My littlest brother: Destaw Getie

Table of Contents

List of Figures

List of Tables

List of Abbreviations

CAF	Caffeine
E.coli	Escherichia coli
DMSO	Dimethyl sulphoxide
FTIR	Fourier Transform Infrared
FWHM	Full width at half- maximum
IR	Infra-red
NIR	Near Infra- red
NPs	Nanoparticles
ROS	Reactive oxygen species
SEM	Scanning electron microscopy
S.aureus	Staphylococcus aureus
UV/Vis	Ultraviolet visible
XRD	X-ray diffraction
ZnO	Zinc oxide
ZOI	Zone of inhibition

Abstract

In this study, the ZnO nanoparticles were synthesised by using salt precursors $ZnCl_2$, $Zn(NO3)_2.6H_2O$ and $Zn(CH3COO)_2.2H_2O$ via a wet chemical method and calcinated at 200 , 300 and 400 ^0c respectively for antibacterial applications. Also, the synthesised ZnO NPs were modified using biologically active compound caffeine. The average crystallite size of the ZnO Nps determined by XRD was about 31.86 nm and 28.09 nm for samples synthesised by $Zn(CH3COO)_2.2H_2O$ and $Zn(NO3)_2.6H_2O$ respectively. The shape of ZnO NPs synthesised from $Zn(NO3)_2.6H_2O$, $ZnCl_2$ and $Zn(CH3COO)_2.2H_2O$ were agglomerated flower-like spherical and rod-like respectively. The variation in size and shape of ZnO NPs is due to the difference in precursors and calcination temperature. The UV-Vis absorption peak of the ZnO NPs was observed at 278 nm, 374 nm and 378 nm for $ZnCl_2$, $Zn(NO3)_2.6H_2O$ and $Zn(CH3COO)_2.2H_2O$ respectively. The vibrational phonon of ZnO observed at 507cm^{-1}, 433 cm^{-1} and 507 cm^{-1} for precursors of $ZnCl_2$, $Zn(NO3)_2.6H_2O$ and $Zn(CH3COO)_2.2H_2O$ respectively confirms the successful production of ZnO nanoparticles. The excitation wavelength of the ZnO NPs synthesised from the precursors $ZnCl_2$, $Zn(NO3)_2.6H_2O$ and $Zn(CH3COO)_2.2H_2O$ were performed at 275 nm, 355 nm and 290 nm respectively. The ZnO NPs showed both an ultraviolet emission band at 325nm, 392 nm and 435 nm due to the electronic transition from conduction band edge to valence band, and visible emission band at 455 nm, 466 nm and 469 nm due to defects that are related to deep level emissions for $ZnCl_2$, $Zn(CH3COO)_2.2H_2O$ and $Zn(NO3)_2.6H_2O$ respectively. The synthesised ZnO NPs were applied for antibacterial activity on S.aureus and E.coli bacteria using disc diffusion agar method. All the three ZnO Nps showed admirable antibacterial activity on S.aureus than the standard antibiotic drugs. Among the three, the ZnO NP synthesised from the precursor $ZnCl_2$ showed excellent antibacterial activity.

1 Introduction

Nanotechnology is currently hot research field in the area of materials sciences due to vast applications. It is an emerging and highly interdisciplinary field which bringing us thrilling novel products and promises to alter the way we live and work in the future. It is also the means of understanding the relationship between the physical property, phenomena and nanomaterials dimensions [1]. The concept of "nano" was first originated by Richard Feynman's 1959 lecture "There's Plenty of Room at the Bottom" in which he wished-for the direct manoeuvring of individual atoms as a more powerful form of synthetic chemistry. However, the term nanotechnology was first defined by Norio Taniguchi of Tokyo University in 1974 to portray the accuracy manufacture of nanomaterials. He defined nanotechnology as the design, synthesis, characterization, exploration, fabrication and application of nanomaterials (1-100 nm) by controlling their size and shape. Simply, it is the application of nanoscience to practical applications mainly for industry and commercial purposes [1, 2].

Nanoscience is a branch of science which deals about nanomaterials that displays significant properties that are not available in bulk materials and exhibit vast applications due to their small size [1]. Nanoparticles are the class of materials and remarkable scientific tools that has been used for various biotechnological, pharmacological and technological uses. They are cornerstones of nanoscience and nanotechnology. Nanoparticles are different from bulk materials due to their small size, higher surface area to volume ratio, crystallographic surface structure, specific magnetic properties and new quantum effects. They also exhibit

unique physical and chemical properties which exist due to the presence of a high concentration of defects like electrical, catalytic, magnetic, mechanical, thermal, or imaging features [3].

Nanoparticles are grouped into organic and inorganic nanoparticles; however inorganic nanoparticles are more applicable due to their ability to withstand harsh processing conditions present in many industries. Nanomaterials may be metals, ceramics, polymers as well as composites. Metal elements have better performance to form a large diversity of oxide compounds used in the fabrication of microelectronic circuits, sensors, piezoelectric devices, fuel cells, coatings for the passivation of surfaces against corrosion [4].

Metal oxide nanoparticles have distinctive interest to researchers because of their multifunctional properties. They display novel and enhanced physical, chemical and biological properties due to their nanoscale dimensions, low melting point, high mechanical strength, high density of corner and random motion. They also show emerging optical, magnetic, electrical and catalytic properties [5]. Among various inorganic metal oxide nanoparticles, ZnO nanoparticles have their own importance due to their vast area of applications. It has tremendous scientific and technological interest [6].

ZnO nanoparticles can be synthesised by using two approaches. Firstly, by "Top Down" method where large objects are modified to give smaller features and secondly, by "Bottom Up" method where small building blocks are produced and assembled into larger structures by controlling the morphology, crystallinity, particle size, and chemical composition. Among these, bottom up method is the most popular and simple due to its low cost and reliability [4].

Zinc oxide is an intrinsic n-type semiconductor material with a chemical formula ZnO [7]. It is a direct-band gap material in which the maximum energy of the valence band and the minimum of the conduction band occur at the same value of the momentum. Oxygen has the highest ionization energy, which leads to a strongest interaction between the Zn3*d*- and O2*p*-orbitals [8]. Due to this strong interaction, ZnO is having a direct wide band gap energy (3.37eV), high exciton binding energy (60 meV), high electron mobility [9], higher breakdown field strength, higher quantum efficiency, non central symmetry and excellent chemical stability. It is nontoxic and naturally occurs as the rare mineral zincite. But, ZnO which used for commercial purposes is produced synthetically. It is transparent to visible range of spectrum and exhibits unique optical, electric conductivity and piezoelectric properties [10]. It also has high electrochemical coupling coefficient, broad range of radiation absorption, biocompatibility, biodegradability and high photostability property [11]. Nowadays, zinc oxide is an interesting topic to researchers due to its significantly unique and essential morphology such as nanorods, nanoflowers, nanowires, nanodendriter and nanoparticles [12, 13].

ZnO is the most significant compound for electronic and optoelectronic applications such as solar cells (anti-reflecting coating and transparent conducting materials), varistors, luminescence, electrostatic dissipative coatings, transparent UV protection films, gas sensors, liquid crystal displays, heat mirrors, surface acoustic wave devices etc due to its high optical transparency and luminescent properties in the near ultraviolet and the visible regions [14,15]. It has a great potential in sunscreens, ointments, creams and lotions due to its ability to reflect the skin deteriorating UV radiation. The powder is widely used as an additive into

numerous materials and products including plastics, ceramics, glass, adhesive, ferrites, sealants, cement, rubber manufacturing, lubricants, batteries, fire retardants, etc. It has been used in food industry for food supplements, breakfast cereals and animal feedstuffs as a source of zinc nutrient [16]. Currently, Zinc oxide nanoparticles have vast applications in various industrial areas due to their exceptional characteristics such as anti-corrosion, ultraviolet filtering, catalytic, low electrons conductivity and excellent heat resistance. They are used in paints, solar cells as window layers electronics, stain-resistant clothing, UV light-emitting devices, photocatalysis, electronics, water filtrations and pharmaceuticals products. They are also used in textile and cosmetics industries due to their higher surface area to volume ratio, high UV absorption and pyroelectric properties [3].

Due to their significant optical, electrical, and magnetic properties ZnO nanoparticles have crucial role in communications, sensing, data storage, optics, transmission, environmental protection, biology, and medicine. They are also used in sunscreens as an ultraviolet- resistant additive and in a range of textile. Zinc oxide nanoparticles have vast biomedical application without coating because of their non-central symmetry, biosafe, less toxicity, antibacterial activity, effective drug delivery, tumour targeting, anti- inflammatory activity, bioabsorption and biocompatibility, imaging features and piezoelectric properties [3]. They show a higher degree for selections of cancer cell with the ability exceed the therapeutic indices of a few universally used chemotherapeutic agents. They also play a very important role in cellular adhesion and uptake due to their high fluorescence and electrostatic nature. ZnO NPs have also great application for antimicrobial activity in food packaging and processing industries because of reactive oxygen species that induced on their surface [16].

Many researchers have been synthesised and characterized zinc oxide nanoparticles, and studied antibacterial activities depend on size, concentration, dimensions and morphology of nanoparticles [17]. The antimicrobial activity of zinc oxide nanoparticles have been studied against Gram-negative bacteria such as *Pseudomonas aeruginosa*, *campylobacter jejuni*, *Escherichia coli* and Gram-positive bacteria such as *Bacillus subtilis* and *Staphylococcus aureus* [18].

On the other hand, there is no research reports on the applications of ZnO NPs synthesised from zinc chloride, zinc nitrate hexahydrate and zinc acetate dihydrate as an inhibitor for *S.aureus* and *E.coli* bacteria. In addition, the modification of the synthesised ZnO NPs using caffeine is not yet investigated.

Therefore, the general objective of this study was synthesis, modify and characterize zinc oxide nanoparticles using different salt precursors (zinc nitrate hexahydrate, zinc chloride, zinc acetate dihydrate) for antibacterial applications.

The specific objectives of this study were: 1. Synthesis agglomerated flower-like ZnO nanoparticles using zinc nitrate hexahydrate. 2. Synthesis spherical ZnO nanoparticles using zinc chloride. 3. Synthesis rod-like ZnO nanoparticles using zinc acetate dihydrate. 4. Modify the surface of ZnO nanoparticles using caffeine. 5. Characterize the ZnO nanoparticles using X-ray diffraction (XRD), Scanning Electron Microscopy (SEM), UV-Vis Spectroscopy, FTIR Spectroscopy and Fluorescence Spectroscopy. and 6. Apply the synthesised ZnO nanoparticles for antibacterial applications.

The thesis is organized as follows: In chapter 1, introduction to nanoscience and nanotechnology, nanoparticles, metal oxide NPs and zinc oxide, general synthesis routes of ZnO nanoparticles, the applications of ZnO NPs and objectives of the study are presented.

In chapter 2, literature reviews related to ZnO NPs are presented. The ZnO NPs, the crystal structures, chemical and optoelectronic properties of ZnO and the synthesis routes of ZnO NPs are discussed. Furthermore, the characterization techniques (XRD, SEM, UV-Vis Spectroscopy, Fluorescence Spectroscopy and FTIR Spectroscopy) of ZnO nanoparticles, modification of ZnO NPs using bioactive compound caffeine and application of ZnO NPs for antimicrobial activities and food packaging are discussed.

In chapter 3, the materials and methods of the study are presented. This chapter has six sections; in the first and the second sections of this chapter, the various chemicals, solvents and apparatus used to carry out this research work are described respectively. In the third, fourth and fifth sections, the methods of synthesis, modification and characterization are presented respectively. In section six, the antimicrobial activity procedures are presented.

In chapter 4, the results and discussions of the thesis are presented. The average crystallite size, SEM images of unmodified and CAF adsorbed ZnO NPs are reported. Moreover, the UV-Vis absorption peak, emission spectra and IR spectra of ZnO NPs are reported. In the final section of this chapter, antimicrobial activities of ZnO NPs are reported.

Finally, the conclusion of the thesis is presented in chapter 5.

2 Literature review

2.1 Zinc oxide nanoparticles

Among various inorganic semiconductor metal oxide nanoparticles, ZnO nanoparticles are the most functional, strategic, promising, and versatile material due to their high surface area to volume ratio, low toxicity, high chemical stability and biocompatibility [19]. They have neutral hydroxyl groups attached to their surface, which theatre a key role in their surface charge behaviour [20]. The physical and chemical properties of zinc oxide nanoparticles depend on their composition, size and shape. Optical property is the most mesmerizing, fundamental attractions and characteristics and functional aspects of ZnO nanoparticle. It is depend on some parameters such as size, shape, surface characteristics, doping and interaction with the surrounding environment or other nanostructures. Due to their optical properties zinc oxide nanoparticles are applicable in optical detector, laser, sensor, imaging, photocatalysis, photoelectrochemistry and biomedicine. The optical property of ZnO nanoparticles is mainly measured by different spectroscopic techniques. Zinc oxide nanoparticles have been used for targeted imaging of cancer cells, sensing, fighting human pathogens, healthcare products and photodynamic therapy due to their nontoxicity because of their magnetic properties. They have a great potential for biological application due to their quantum effects which can affect the chemical reactivity and other physical and chemical properties, and the similarity of nanoparticles and biomolecules in dimension. The ZnO nanoparticles have useful applications in textile industry since ZnO coating is more air permeable and efficient UV-blockers compared with any other semiconductor material [21]. ZnO NPs have more toxic effects on bacteria and fungi due to some factors like light

intensity, surface chemistry and particle morphology. However, they have minimal effect on human cells [3].

2.2 Crystal structures of ZnO

Zinc oxide has three crystal structures such as hexagonal wurtzite, cubic zinc blende and cubic rocksalt. Among these, wurtzite crystalline structure is the most stable phase at ambient conditions. In this structure every zinc atom is tetrahedrally coordinated with four oxygen atoms. It has lattice parameters, a = 0.32495 nm and c = 0.52069 nm, ratio of c / a =1.6023, which is similar to the ideal value of hexagonal cell *c/a* = 1.633. It belongs to the space group of $P6_3mc$ and is characterized by two interconnecting sublattices of Zn^{2+} andO^{2-}. The cubic rocksalt is observed only at relatively high pressures ~10 GPa. The tetrahedral symmetry of wurtzite structure makes an imperative role for the polarity of ZnO that arises along the hexagonal axis. The polar symmetry of ZnO along the hexagonal axis results piezoelectricity, pyroelectricity and spontaneous polarization. Since ZnO has sensitive lattice constants to the presence of structural point defects (oxygen vacancies and interstitial Zn ions act as donors in its lattice) and extended defects (threading/planar dislocations), it has an n-type nature. These structural point and extended defects are commonly found in ZnO resulting in a non-stoichiometric compound $Zn_{1+d}O$ with excess zinc. They are responsible for visible photoluminescence [9, 10, 11]. Fig 2.1 shows crystal structures of ZnO.

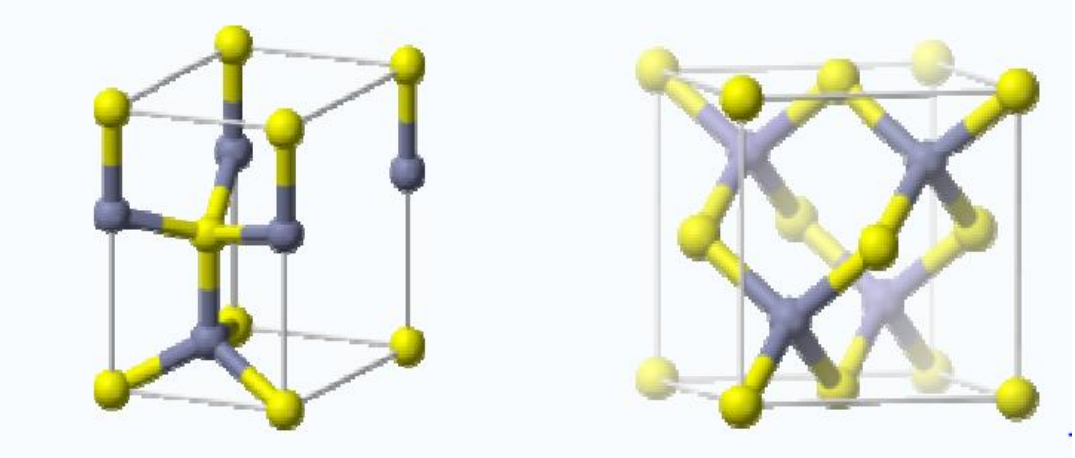

a). Hexagonal wurtzite structure b). Cubic zinc blende structure

Figure 2.1: Crystal structures of ZnO [10]

2.3 Chemical properties of ZnO

Pure ZnO occurs as a white powder usually called as white zincite or mineral zincite. Because crystalline ZnO is thermo-chromic, its color is changing from white to yellow when it is heated in air. It also reverts to white on cooling due to a very small loss of oxygen at high temperature to form the non-stoichiometric $Zn_{1+x}O$. Since zinc oxide is an amphoteric oxide, it is insoluble in water and alcohol, but in most acids like hydrochloric acid and in alkalis. The solubility of ZnO in hydrochloric acid and alkalis, sodium hydroxide, are described according to equation (2.1).

$$ZnO + 2HCl \rightarrow ZnCl_2 + H_2O \qquad 2.1$$

$$ZnO + 2NaOH + H_2O \rightarrow Na_2[Zn(OH)_4]$$

ZnO forms cement like material which are used in dentistry when reacted with phosphoric acid and a strong aqueous solution of zinc chloride. It produce carboxylates like asoleate or stearate when react with fatty acids in oils [10, 11].

2.4 Optoelectronic properties of ZnO

ZnO shows a better optoelectronic property because of its large exciton binding energy (60 meV) which could be attended at and above room temperature due to excitonic recombination. The optical properties of ZnO are heavily influenced by the energy band structure and lattice dynamics. The processes of optical absorption and emission have been influenced by an extrinsic transition called bound exciton. This bound exciton is related to defects which are responsible for creating discrete electronic states in the band gap. Exciton can be bound with neutral or charged donors and acceptors and it depends on the band structure of semiconductor material. Thus bound exciton do not requires traps to localize carriers and recombines with high efficiency. Zinc oxide films which made from single crystal can be applied for modulation of UV radiation due to its directionally dependent optical property. It is also used for different electronic application due to its high breakdown stress and high saturation velocity. Due to its higher radiation, chemical, and thermal resistance, ZnO is used to form transparent contacts of solar cells. Fluorescence spectra of ZnO nanowire shows increase of green emission intensity with a decrease of nanowire diameter and continuous reduction of diameter of ZnO nanowire gives quantum size effect and due to this size confinement exciton binding energy is enhanced. The performance of optoelectronic devices have been influenced by transport characteristics and interaction of phonon with free carrier [22].

2.5 Synthesis routes of ZnO nanoparticles

2.5.1 Top-down method

Top-down method is a physical method in which a microcrystalline or bulk material has been broken down again and again in to small pieces with various lithographic techniques like grinding, milling etc. The microcrystalline or bulk material becomes like a powder, which is in the form of nanomaterials. All the solid state routes fall in to this category including, Mechanical alloying, equal channel angular pressing (ECAP), high-pressure torsion (HPT), accumulative roll bonding (ARB), nanolithography, etc [4].

2.5.2 Bottom-up method

Bottom- up method is a chemical method where nanomaterials are building up from bottom to upwards. This means that adding (self-assembling) a very small atoms or molecules up to require size. The two vital processes in the bottom-up method are nucleation and growth. Nucleation is the first step of phase transformation where an aggregate of atoms are formed. All techniques that start with liquid and gas as the starting material fall in to this category including, physical vapour deposition (PVD), chemical vapour deposition, spray conversion processing, sol-gel process, wet chemical method and self-assembly [4]. Among these, wet chemical method is the most simple and popular method due to its low cost, reliability and environmental friendly synthetic routes. It also provides rigorous control of the size and shape of the nanoparticles [14].

2.6 Characterization techniques of ZnO nanoparticles

In order to apply zinc oxide nanoparticles for any of applications characterization should be carried out after synthesis of the material. Several physical techniques have been developed to characterize the size, morphology and other remarkable properties of zinc oxide nanoparticles. The most commonly used characterization techniques are X-ray diffraction (XRD), Scanning Electron Microscopy (SEM), UV-visible Spectroscopy, Fluorescence Spectroscopy and FTIR Spectroscopy. The detail information about these techniques is explained as follows.

2.6.1 X-ray diffraction (XRD)

X-ray is an energetic electromagnetic radiation appearing at the region between gamma-rays and ultraviolet, with wavelength comparable with the size of an atom. When X-rays interact with a crystalline substance (phase), one gets a diffraction pattern. The reflection of incident monochromatic X-ray from successive planes of crystal lattices when the difference between the planes of complete number n of wavelengths leads to famous Bragg's law [23]. The Bragg's law can be described according to equation (2.2).

$$n\lambda = 2d \sin\theta \qquad 2.2$$

Where n is an integer 1, 2, 3..., λ is wavelength in nanometer, d is interatomic spacing and θ is the diffraction angle in degrees.

XRD is a non destructive analytical technique which does not require intricate sample preparation. Mostly it is used for the fingerprint characterization of crystalline materials and the efficient determination of their structure, chemical composition and physical properties. It

is a very functional and powerful tool to structural characterization including how the atoms pack together in the crystalline state and what the interatomic distance and angle are etc [24].

XRD can also used to characterize nanoparticles such as ZnO NPs. It determines the average crystallite size of ZnO NPs. A great advantage of X-ray powder diffraction is that it requires virtually no sample preparation, in comparison to other characterization techniques. The sample can be either in the form of smear or compact flat pack or a capillary and is exposed to monochromatic beam of x-ray and the diffracted beam intensity is collected in a range of angles (2θ) with respect to the incident beam. The intensity corresponding to a constructive interference of the diffracted beam from a crystallographic plane is observed as peak, corresponding to the Bragg angle (θ). A powder diffraction pattern contains information on phases present (peak positions), phase concentrations (peak heights), structure, degree of crystallanity or amorphous content (background hump) and crystallite size/strain (peak widths/broadening).The width of the peaks in a particular phase pattern provides an indication of the average crystallite size. Large crystallites give rise to sharp peaks, while the peak width increases as crystallite size decreases. Crystallite size does not equal the size of the particle, as one particle can be a conglomerate of several crystallites. Peak broadening also occurs as a result of variation in d-spacing caused by microstrain. The positions of the peaks provide an accurate fingerprint of the crystal structure of the nanocrystals. The average crystallite size of the ZnO nanoparticles can be obtained from the line broadening using Debye Scherer formula [23, 24] according to equation (2.3).

$$D = \frac{0.9\lambda}{B \cos \theta} \qquad 2.3$$

Where D is average crystallite size, λ is wavelength of incident beam (1.5406Å), β is full width at half-maximum (FWHM) in radians and θ is scattering angle in degree.

The lattice constants a' and 'c' and the spacing 'd_{hkl}' for wurtzite structure of ZnO can be calculated according to equation (2.4) and (2.5). Figure 2.2 shows the X-ray diffraction of materials in accordance with Bragg's law.

$$a = \sqrt{\frac{1}{3}} \frac{\lambda}{\sin \theta} \text{ and } c = \frac{\lambda}{\sin \theta} \qquad 2.4$$

$$d_{hkl} = \frac{ac}{2} \sqrt{\frac{3}{c^2(h^2+hk+k^2)+3\frac{(al)^2}{4}}} \qquad 2.5$$

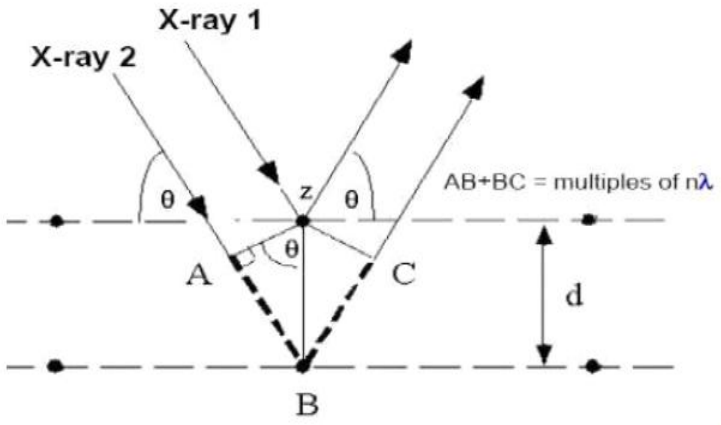

Figure 2.2: X-ray diffraction of materials in accordance with Bragg's law [24]

2.6.2 Scanning Electron Microscopy (SEM)

Scanning electron microscopy (SEM) is a microscopic instrument which gives detail information about size, external morphology (texture), microstructure, composition, topography, and crystal orientation of ZnO nanoparticles. Electrons are thermoionically emitted from a tungsten or lanthanum hexa boride cathode and are accelerated towards an anode; alternatively electrons can be emitted via field emission. The electron beam, which has an energy ranging from a few hundred eV to 100 KeV, is focused by one or two condenser lenses in to a beam. Characteristic X-rays are emitted when the primary beam causes the ejection of inner shell electrons from the sample and are used to determine the elemental composition of the sample. As most biological specimens are made up of non-dense material the amount of secondary electrons produced is too low to be of much use in creating an image and therefore they are usually coated with a very fine layer of a metal which readily produces secondary electrons. The back scattered electrons emitted from the sample can be used alone to form an image or in composition with the characteristic X-rays. These signals are monitored by photomultiplier tubes and magnified. An image of the investigated microscopic region of the specimen is observed in cathode ray tube [25].

2.6.3 UV-Visible Spectroscopy

UV-visible Spectroscopy is the type of absorption spectrophotometer which involves the excitation of electrons present in the molecule from ground state to excited state. It is the most reliable and accurate analytical method which used to measure scanning or transition of electron and optical properties of materials. Absorption spectrophotometer is the analytical technique in which compounds absorb light of radiation of a specific wavelength. A

spectrophotometer is an instrument used to measure the transmittance and absorbance of a sample as a function of the wavelength of electromagnetic radiation. Absorbance (A) is the amount of light that is absorbed by a sample, while transmittance (T) is the amount of light transmitted through a sample. Transmittance also defined as the ratio of the light energy transmitted by the sample I to the energy transmitted by the reference blank I_o [26]. Mathematically, it is expressed according to equation (2.6).

$$T = \frac{I}{Io} \qquad 2.6$$

The absorbance of light in a molecule in the solution can be expressed by Beer Lambert's law according to equation (2.7).

$$A = -\log_{10} T = \log \frac{Io}{I} \qquad 2.7$$

Where A is absorbance in arbitrary unit, T is transmittance, I_o is the intensity of the reference beam and I is the intensity of the sample beam.

UV-Vis spectroscopy is almost entirely used for quantitative analysis in which the estimation of the amount of a compound known to be present in the sample solution. The components of UV-Vis spectroscopy are light source that generates a broad band of electromagnetic radiation, monochromater (wavelength selector), sample holder, detector to measure the intensity of radiation and computer (read signal). The absorption spectra of atoms, molecules, or ions are generated when a beam of electromagnetic energy or light is passed through a sample, and absorbs a portion of the photons of electromagnetic energy passing through the sample [27].

UV-Vis spectroscopy can also used to characterize the nanoparticles such ZnO nanoparticles. It measures the absorption peak of ZnO nanoparticles, which occurred due to

transition or scanning of electron from valence band to conduction band. When an electron gets some amount of photon energy from UV or visible light, it is jumping from valence band (lower energy) to conduction band (higher energy). It is the peculiar property for ZnO. The absorption peak is depend on some factors like selection of wavelength, nature of the solvent, band gap, oxygen deficiency, size and structure of the nanoparticles, surface roughness, impurity centres, PH of the solution and temperature. Generally, as it was reported in several literatures, the UV-Vis absorption peaks of ZnO NPs are found between 350 nm- 380 nm. However, the UV-Vis absorption spectrum of ZnO NP synthesis using the salt precursor zinc chloride is in the range of 270 nm- 290 nm [27, 28].

The band gap energy, the energy required for the transition of electron from a state of lower energy (E_1) to state of higher energy (E_2) is equivalent to the energy of electromagnetic radiation (photon energy) that causes transition [26]. It is given by equation (2.8).

$$\mathrm{Eg} = \mathrm{E2} - \mathrm{E1} = \frac{\mathrm{hC}}{\lambda} \qquad 2.8$$

Where Eg is band gap energy, h is Planck's constant, C is speed of light and λ is related wavelength of the sample.

2.6.4 Fourier Transform Infrared (FTIR) Spectroscopy

FTIR Spectroscopy is a non-destructive and highly flexible instrument which able to measure bond vibrational motions of atoms in molecules. It is a powerful technique for chemical characterization, identification of functional groups and used to achieve information regarding the attachment of the capping agents. In recent time, it has been replaced dispersive instruments for most applications due to its superior speed and sensitivity [29].

The three basic spectrometer components of FTIR spectroscopy are radiation source, interferometer and detector. It uses a beam of infrared light to analyze the structure of organic compounds, identify unknown materials, and determine the quality or consistency of a sample and the amount of components in a mixture [30]. FTIR analyze a wide range of materials in bulk or thin films, liquids, solids, pastes, powders, fibers, and other forms. Its spectra of pure compounds are generally so unique that they are like a molecular "fingerprint" [31]. Vibrational motion of atoms in a molecule is influenced by the masses of atoms, their geometrical arrangement and strength of their chemical bonds. There are IR and Raman spectra, which are the results of transition between quantized vibrational states and provide a complementary image of molecular vibrations. Both IR and Raman spectra involves IR radiation [30]. Specific types of chemical bonds or functional groups can be identified by infrared spectroscopy based on their unique absorption signatures. Identification of functional groups is the cornerstone of IR spectroscopy, which produces broad absorptions. Molecules absorb resonant frequencies that are characteristic of their structure. This means the frequency of the absorbed radiation matches the frequency of the bond or group that vibrates and the detection of energy is done on the basis of shape of the molecular potential energy surfaces, the masses of the atoms, and the associated vibronic coupling. IR encompasses a spectral region from red end of visible spectrum (12500 cm^{-1}) to 10 cm^{-1} region in the electromagnetic spectrum. It is the most influential tool to identify compounds by matching spectrum of unknown compound with reference spectrum (finger printing) and functional groups in unknown substances. IR is commonly divided into near IR (12500 to 4000 cm^{-1}), mid IR (4000 to 400 cm^{-1}) and far IR (400 to 10 cm^{-1}). Among these, mid IR

(4000 to 400 cm-1) spectra region is the most significance and richest region in chemical information due to the occurrence of the most fundamental molecular vibrations [30, 31].

FTIR spectroscopy also used to characterize ZnO NPs to investigate their vibrational motions. It gives detail information about the surface chemistry of ZnO nanoparticles and functional groups attached to the zinc oxide nanoparticles surface. These functional group shows various FTIR pattern than those of free groups. Zinc oxide generally gives vibrational phonon in fingerprint region from 400 cm^{-1}- 600 cm^{-1} arising from inter-atomic vibrations. The IR spectra of ZnO NPs greater than 600 cm^{-1} is due to some other carboxylic and hydroxyl groups like O-H, C=O, C-H, C-O, which are attached to zinc oxide nanoparticles during synthesis [32].

2.6.5 Fluorescence Spectroscopy

Fluorescence spectroscopy is a rapid, sensitive and selective characterization method. It is a contactless and non-destructive method to investigate the electronic structure of materials. It is also a type of electromagnetic spectroscopy that analyzes fluorescence from a sample using a beam of ultraviolet light. This beam of light excites the electrons in molecules of certain compounds and causes them to emit light. In the single molecule fluorescence spectroscopy, intensity fluctuations from the emitted light are measured from either single fluorophores or pairs of fluorophores [33].

Bulk metal does not usually possess photoluminescent properties due to the absence of band gaps in the atomic solid-state structure. Fluorescence spectroscopy measures the intensity of photons emitted from a sample, an excitation spectrum and emission spectrum. The three basic parts of fluorescence spectroscopy are source of light, sample holder and detector. Photons impinge on the excitation monochromater, which selectively transmits light

in a narrow range centered about the specified excitation wavelength. The transmitted light passes through adjustable slits that control magnitude and resolution by further limiting the range of transmitted light. The filtered light passes into the sample cell causing fluorescent emission by fluorophores within the sample. Emitted light enters the emission monochromater, which is positioned at a 90º angle from the excitation light path to eliminate background signal and minimize noise due to stray light. Again, emitted light is transmitted in a narrow range centered about the specified emission wavelength and exits through adjustable slits. Spectral resolution and signal to noise is directly related to the selected slit widths. The particle cannot emit energy at the place where it was absorbed [33, 34].

Fluorescence spectroscopy also used to characterize nanoparticles such ZnO NPs. This technique involves measuring the energy distribution of emitted photons after optical excitation of ZnO nanoparticles. Since ZnO is a semiconductor, free electrons are there in the conduction band and holes are in the valence band. When electrons make a transition from ground state to excited state because of some photon energy which is emitted from the source, energy is absorbed. While this electron came back to valence band, emission is occurred i.e energy is emitted. The emission spectra of ZnO nanoparticles have been exceed their absorption spectra due to their semiconducting properties. This is implies when some amount of radiation (photon) is supply, electrons are climb from valence band (lower energy) to conduction band (higher energy), and when it came backs to valence band (lower energy) from conduction band (higher energy), the wavelength is greater since photon energy is inversely proportional to wavelength. Generally, ZnO exhibits two kinds of emissions: one is at ultraviolet near band-edge emission and the other a visible deep level emission with a peak in the range from 450 to 700 nm. The UV emission is related to the electronic transition from

conduction band edge to valence band. The Visible emission spectra is caused by the transition from deep donor level to valence band due to oxygen vacancies and by the transition from conduction band to deep acceptor level due to impurities and defect states [34].

2.7 Modification of ZnO nanoparticles

ZnO NPs can be modified using inorganic, organic and polymer materials. Modification of zinc oxide nanoparticles by inorganic ions have been change surface area and size of the particles, reduced the photocatalytic action of the oxide and improve their dispersion degree. The other research studies indicated the modification of zinc oxide nanoparticles using organic compounds such as carboxylic acids (such as stearic, tartaric, maleic, propanoicetc.) makes it possible to introduce characteristic groups onto the surface of the ZnO and to alter its physicochemical properties, increase the compatibility of ZnO with organic matrix, reduce aggregation of particles, enhancing long term stability in organic materials and to improve the unique electrical, thermal and optical properties of ZnO NPs. Studies of ZnO NPs modified with carboxylic acids (wet modification) have shown that they do not significantly affect the morphological/dispersive or porous properties of zinc oxide [35].

2.8 Applications of ZnO nanoparticles

2.8.1 Antimicrobial applications of zinc oxide nanoparticles

The real progress towards the use of ZnO NPs as an antimicrobial agent was started in 1995, when Sawai and his colleagues found that MgO, CaO and ZnO nanoparticle powders had antimicrobial activities against some bacteria strains [36]. Now a days, Zinc oxide is listed as a generally recognized as safe (GRAS) material by the Food and Drug Administration and is

used as food additive. Zinc is an essential micronutrient which used for intensification, improvement and health in humans and animals [16].

Invitro antibacterial activity of ZnO nanoparticles have been performed by different methods, but the most one is broth dilution method which is followed by colony count. This method consists of determining the number of doable bacteria by plating, in appropriate agar medium, serial dilutions of intention microorganisms incubated in culture broths containing ZnO nanoparticles at different concentrations and appropriate time/temperature conditions. The antibacterial activity of ZnO nanoparticles have been tested against some gram-positive *Bacillus subtilis* and *Staphylococcus aureus*; and gram-negative bacteria *Pseudomonas aeruginosa*, *Campylobacter jejuni* and *Escherichia coli* [37]. E.coli has higher susceptibility to ZnO nanoparticles than S. aureus. The higher resistance of S.aureus to ZnO nanoparticle than *E.coli* is due to the fact that *S. aureus* contains carotenoid pigments, which promote a greater oxidant resistance and due to the presence of potent detoxification agents such as antioxidant enzymes, particularly catalase [38].

Gram-positive bacteria have more sensitivity to reactive oxygen species (ROS) than Gram-negative bacteria due to two main reasons. The first is structural difference in bacterial membrane, i.e Gram-positive bacteria have a membrane, which surrounds the cell, and a cell wall primarily made up of peptidoglycan layer, teichoic and lipoteichoic acids. Gram-negative bacteria have more complex cell wall due to the presence of an outer membrane, which is composed mainly of lipopolysaccharide (LPS), in addition to a thin peptidoglycan layer. This outer membrane acts as a permeability barrier; this result the absorption of ROS into the cell is reduced [39]. The second one is polarity difference of cell membrane, since the membrane of *S.aureus* has more positive charge than *E.coli*, which allows a greater

penetration level of negatively charged free radicals such as hydroxyl radicals, superoxide and peroxide ions causing damage and cell death in *S.aureus* at concentrations below that required to cause the same effect in *E.coli*. The antimicrobial activity of ZnO nanoparticle is affected by some factors like size of nanoparticle, concentration and surface area, but strongly influenced by their size. This implies that the antimicrobial activity of ZnO on *E.coli* and *S.aureus* has been improved with diminution of particle size due to an increase in the surface area to volume ratio, which results in the increased reactivity of ZnO nanoparticle surface. This is the fact that a larger surface area will result in more ROS on the surface of ZnO and, therefore, in a greater antibacterial activity of smaller nanoparticles. The toxicity of ZnO nanoparticles could be depend on their shape due to the increase proportionality of interaction forces of lengthwise-oriented nanoparticles to their lengths [40].

The three mechanisms for the antimicrobial activity of ZnO nanoparticles are the release of antimicrobial ions, interaction of nanoparticles with microorganisms [41] and the formation of ROS by the effect of light radiation [17]. Many researchers have been reported the occurrence of ROS is the main mechanism [17, 37, and 41]. When ZnO nanoparticles activate by visible and UV light, ROS is generating on their surface. Electrons move from the valence band (vb) to the conduction band (cb) of the ZnO nanoparticle due to the higher incident radiation with photon energy of ZnO compared to its band gap energy (~3.37eV). As a result a positive area, an electron hole (h+) in the valence band and a free electron (e−) in the conduction band is formed [42]. The electron hole (h+) reacts with H_2O molecules (from the suspension of ZnO) separating them into •OH and H^+; and O_2 molecules dissolved in the medium are transformed into superoxide anion radicals (O_2^-), which in turn react with H^+ and generate (HO_2•). Consequently, this species collides with electrons producing hydrogen

peroxide anions (HO_2). Thus, the hydrogen peroxide anion reacts with hydrogen ions to produce H_2O_2 molecules [37].

2.8.2 Zinc oxide nanoparticles in food packaging application

Zinc oxide nanoparticles are also used for the control of food borne pathogens and providing safety and maintaining quality of food and also for food packaging. Food packaging is a type of active packaging which interacts with products (the headspace inside) to reduce, inhabit or retard the growth of microorganisms that may present on food surface. Organic compounds like organic acids, essential oils, bacteriocins and enzymes like lysozyme are strong antimicrobial agent and tested for their potential application in polymeric matrices as antimicrobial packaging at low concentration, but they are sensitive to processing conditions such as high temperature and pressure[43]. ZnO nanoparticles are used for antimicrobial activity in food packaging and processing industries due to their high surface area to volume ratio, unique physical and chemical properties, their stability in extreme condition such as at high temperature and pressure and long shelf-life. They have higher potential in food packaging and preservation applications because of their biosafe, less toxicity, long shelf life and biocompatibility [6].

3 Materials and Methods

3.1 Chemicals and solvents

The chemicals used for the synthesis and modification of zinc oxide nanoparticles are zinc nitrate hexahydrate ($Zn(NO3)_2.6H_2O$) (Himedia, India), sodium hydroxide (NaOH) (Alpha chemika, India), zinc chloride($ZnCl_2$) (Neolab, India), zinc acetate dihydrate ($Zn(CH3COO)_2.2H_2O$) (Uni-Chem, India), caffeine ($C_8H_{10}N_4O_2$) (Sigma-Aldrich, Germany). And the solvents are deionized water, nitric acid and di-methyl sulphoxide (DMSO). All the chemicals are analytical grade and do not undergo further purification.

3.2 Apparatus

The apparatus used for synthesis and characterize ZnO NPs are magnetic stirrer with hot plate, whatman filter paper, mortar and pestle, glass rod, spatula, analytical balance with accuracy 0.0001g, different sizes of beakers and sample holders, crucible, puddle, drying oven , furnace and 1cm quartz cuvette.

3.3 Synthesis Methods

During synthesis of ZnO NPs the main parameters such as, size of the particle, chemical composition, crystalline structure and morphology must be controlled [4]. In this study, wet chemical method was used for the preparation of ZnO nanoparticles. The chemicals required for this method are easily accessible and inexpensive.

3.3.1 Synthesis of Agglomerated flower- like Zinc Oxide Nanoparticles

About 12 gm of $Zn(NO3)_2.6H_2O$ was dissolved in 100 ml of deionized water in a beaker and stirred for 25 minutes using magnetic stirrer. The resulting solution was heated under constant stirring, at the temperature of 70 ^{0}c. Subsequently, 3.2 gm of NaOH was also dissolved in 30 ml of deionized water in a separate beaker and stirred for 10 minute. After this, a solution of NaOH was slowly (drop by drop) added into the beaker containing the $Zn(NO3)_2.6H_2O$ solution under stirring condition. The suspension formed with the dropping of NaOH alkaline aqueous solution to the $Zn(NO3)_2.6H_2O$ solution was kept stirred for two hours at the temperature of 70 ^{0}c. The mixed solution was settled under normal air condition for few hours, and filtered using whatman filter paper. The filtered sample was dried in oven at 160 ^{0}c for 31/2 hours, and calcinated at 300 ^{0}c for 5 hours in a muffle furnace. Finally, the material was grinded using mortar and pestle.

3.3.2 Synthesis of Spherical Zinc Oxide Nanoparticles

About 20 gm of zinc chloride was dissolved in 100 ml of deionized water in a beaker and stirred for 45 minutes using magnetic sterrier at the temperature of 90 ^{0}c. Similarly, 7.27 gm of NaOH was dissolved in 100 ml of deionized water in a separate beaker and stirred for 20 minutes. 58 ml solution of sodium hydroxide was added to the beaker containing $ZnCl_2$ solution with constant stirring. The aqueous solution turned into a milky white colloid without any precipitation. The reaction was allowed to proceed for 2 hour after complete addition of sodium hydroxide. The solution was allowed to settle and filter using whatman filter paper. The filtered sample was allowed to dry in oven at 160 ^{0}c for 7 hours, and

calcinated at 200 ^{0}c for 2 hours in a muffle furnace. Finally, the material was grinded using mortar and pestle.

3.3.3 Synthesis of Rod- like Zinc Oxide Nanoparticles

About 15 gm of $Zn(CH3COO)_2.2H_2O$ was placed into a crucible and calcinated at 400 ^{0}c for 12 hours in a muffle furnace without any special atmospheric condition. Finally, the material was grinded using mortar and pestle.

3.4 Modification of ZnO nanoparticles with caffeine

About 4 gm of zinc oxide nanoparticles and 1.5 gm of caffeine was dissolved in 60 ml of di-methyl sulphoxide in a beaker. The mixed solution was stirred for 5 hours using magnetic sterrier at the temperature of 40 ^{0}c. After this, the solution was settled under normal air condition and filtered using whatman filter paper. Finally, the filtered sample was dried in oven for 8 hours at 160 ^{0}c.

3.5 Methods of characterization

3.5.1 XRD characterization

The X-ray powder diffraction patterns of the ZnO NPs were recorded using X-ray Diffractometer (PANalytical XPERT-PRO Diffractometer) equipped with nickel filtered Cu-$K\alpha_1$ radiation (λ= 1.5406 A^0) operating at 45 KV and 30 mA. The data have been collected in the scan range (2θ) from 10^0 -100^0 [45].

3.5.2 SEM characterization

The morphological feature of the modified and unmodified ZnO NPs were determined by using Scanning Electron Microscopy (SEM), using electron beam energy of 10 KV and 15

KV. The ZnO NP powder is mounted on a sample holder followed by coating with a conductive metal. Then, the sample was scanned with focused fine beam of electrons. The surface characteristics of the sample were obtained from the secondary electrons emitted from the sample surface.

3.5.3 UV- Vis spectroscopy characterization

The UV-Vis absorption peaks of ZnO NPs were recorded with UV-Vis spectroscopy (PerkinElmer, Lambda 950 UV/VIS/NIR Spectrophotometer) in the wavelength region of 260 nm - 600 nm at room temperature. The ZnO nanoparticles were dissolved in DMSO and its absorbance measured using 1cm quartz cuvette. The ASC files of the measured spectra were collected by computer which interfaced with the instrument. Finally, the absorption spectra of ZnO NPs were analyzed using origin 8 software.

3.5.4 Fluorescence spectroscopy characterization

The emission spectra of ZnO NPs were measured with fluorescence spectroscopy (Fluoromax-4 Spectrofluorometer) at room temperature. The samples was dissolved in di-methyl sulphoxide (DMSO) and stirred until it dissolved. The emission spectra of the sample were measured by 1 cm quartz cuvette. The excitation wavelength of the samples were performed at 310 nm, 275 nm and 355 nm for salt precursors of $Zn(CH3COO)_2.2H_2O$, $ZnCl_2$ and $Zn(NO3)_2.6H_2O$ and emission wavelength in the wavelength region of 300 nm- 500 nm respectively. The slit width of the instrument was adjusted to 5 nm.

3.5.5 FTIR spectroscopy characterization

The vibrational phonon and the quality of ZnO NPs were also characterized by Fourier transform infrared spectroscopy (PerkinElmer, Spectrum 65 FTIR) in the wavenumber region of 4000-400 cm^{-1} according to the procedures reported by [31]. The ZnO NPs spectra measurements were performed by putting the powder ZnO NPs on KBr pellet.

3.6 Antibacterial activity procedures

The antibacterial activity of the zinc oxide nanoparticles on *S.aureus* and *E.coli* bacteria were tested by disc diffusion agar method according to the procedures reported by [45]. *S.aureus* and *E.coli* bacteria were grown aerobically in nutrient broth for 24 hours at 37 ^{0}c before using as target organisms. About 300 mg, 450 mg and 600 mg of each ZnO nanoparticles synthesised from the salt precursors $ZnCl_2$, $Zn(NO3)_2.6H_2O$ and $Zn(CH3COO)_2.2H_2O$ were dispersed separately in 30 ml of DMSO and stirred for 2 hours using magnetic sterrier. Filter paper discs (4 mm in diameter) were soaked so that concentrations (10 mg/ml, 15 mg/ml and 20 mg/ml) of the ZnO nanoparticles solution. Control experiments were also carried out in the presence of known standard antibiotic drug (vancomycin). The standard antibiotic drugs and the null filter paper disc were used as control positive and control negative respectively. After inoculation and cultivation of *S.aureus* and *E.coli* target bacteria on top of Mueller Hinton agar, standard antibiotic drug and discs were placed in selected area on different plates. Finally, the diameters of the inhibition zones were measured in millimeters after 24 hour incubation times.

4 Results and Discussion

4.1 XRD patterns of ZnO nanoparticles

Figure 4.1 a-b shows the XRD pattern of unmodified ZnO nanoparticles synthesised using $Zn(NO3)_2.6H_2O$ and $Zn(CH3COO)_2.2H_2O$ respectively. The diffraction peaks of the two ZnO NPs correspond to (100), (002), (101), (102), (110), (103), (112) and (201) planes ((JCPDS file No. 36-1451). The average crystallite size of the ZnO NPs calculated using Eq (2.3) was about 31.86 nm and 28.09 nm for salt precursors of zinc acetate dihydrate and zinc nitrate hexahydrate respectively. The variation in the diffraction pattern and average crystallite size among the ZnO NPs may due to the variation of precursors and calcination temperature. As the temperature increases, the particle size also increase even the precursors are different. All ZnO NPs possess wurtzite crystalline structure with lattice parameters (a= 0.3233 nm and c=0.5606 nm) [48]. There is an impurity on ZnO NPs synthesised from $Zn(NO3)_2.6H_2O$. The summary of the XRD analysis of unmodified ZnO NPs synthesised from $Zn(CH3COO)_2.2H_2O$ and $Zn(NO3)_2.6H_2O$ is given in Table 4.1 a-b respectively.

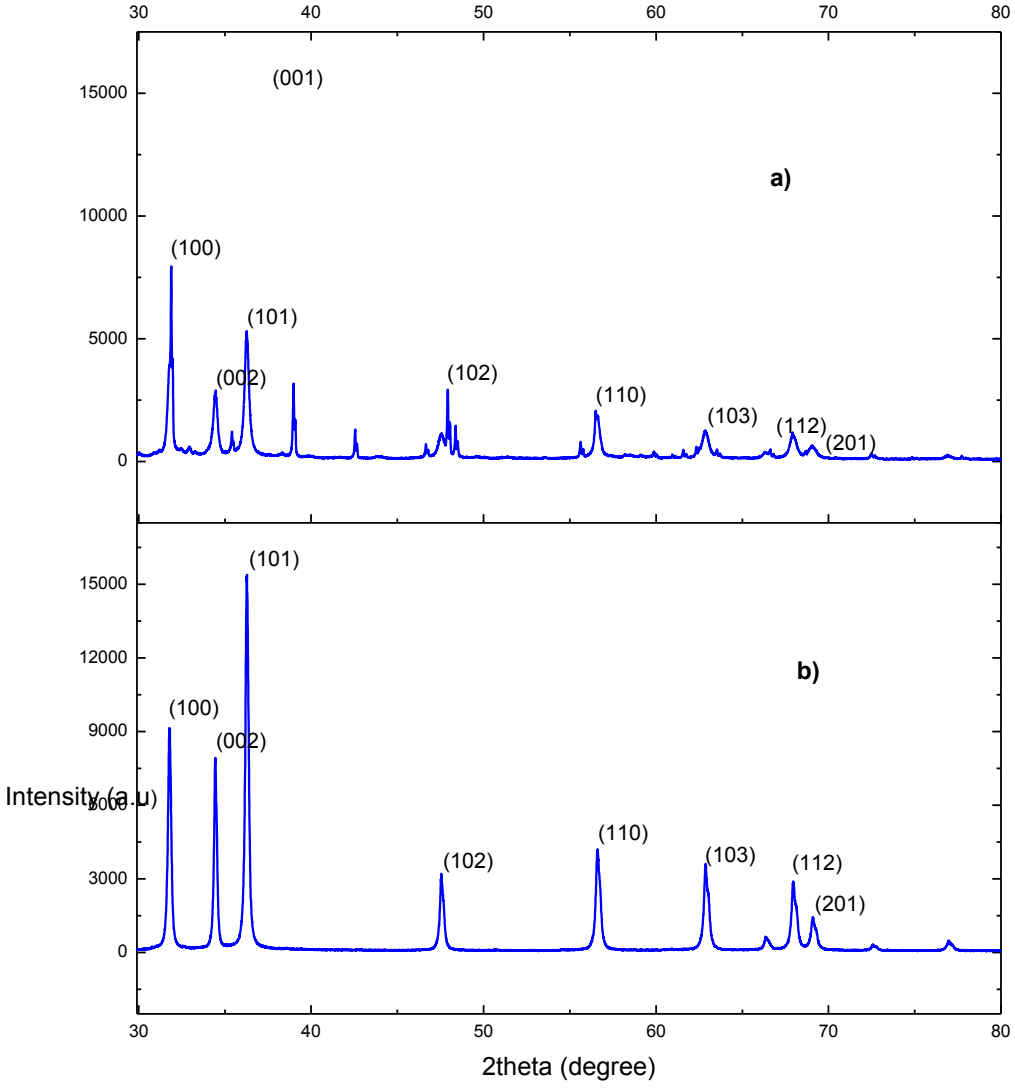

Figure 4.1: XRD pattern of unmodified ZnO nanoparticles synthesised using a) zinc nitrate hexahydrate and b) zinc acetate dihydrate

Table 4.1: The X-ray diffraction parameters and crystallite size of unmodified ZnO nanoparticles synthesised using a) zinc acetate dihydrate and b) zinc nitrate hexahydrate.

a)

hkl	**2θ(degree)**	**FWHM(degree)**	**Crystallite size (nm)**	**D(nm)**
100	31.938	0.22264	37.13	31.86
002	34.598	0.20203	41.20	
101	36.247	0.22781	36.71	
102	47.546	0.28489	30.59	
110	56.536	0.31917	28.27	
103	62.845	0.34739	26.81	
112	67.835	0.35583	26.91	
201	69.154	0.35376	27.28	

b)

hkl	**2θ(degree)**	**FWHM(degree)**	**Crystallite size(nm)**	**D(nm)**
100	31.897	0.23954	34.50	28.09
002	34.453	0.27754	29.98	
101	36.226	0.28338	29.51	
102	47.917	0.25531	34.06	
110	56.556	0.34524	26.14	
103	62.927	0.39805	23.41	
112	67.934	0.41377	23.17	
201	69.135	0.40131	24	

4.2 SEM analysis of the modified and unmodified ZnO nanoparticles

Figure 4.2 a- c shows the SEM micrographs of the modified and unmodified ZnO NPs synthesised using $Zn(NO3)_2.6H_2O$, $Zn(CH3COO)_2.2H_2O$ and $ZnCl_2$ respectively. The morphology of unmodified ZnO nanoparticle synthesised from $Zn(NO3)_2.6H_2O$ was agglomerated flower(Fig 4.2a). The morphology of unmodified and modified ZnO nanoparticle synthesised from $Zn(CH3COO)_2.2H_2O$were rod-like and cotton flower-like respectively(Fig 4.2b). Similarly, the morphology of unmodified ZnO nanoparticle synthesised from $ZnCl_2$ was spherical. The shape of modified ZnO NP synthesised from $ZnCl_2$ was not determined, since grains have no boundary as a result of coalescence of grains (Fig 4.2c). SEM micrographs of the ZnO NPs have different shape and size as shown in Fig 4.2 a-c. The variation of the shape of the ZnO NPs is due to the difference in their precursor, calcination temperature and size [44]. The micrograph shows uncoated ZnO NPs are more aggregated and compressed. By contrast, in Fig 4.2 a-c below, the modified ZnO nanoparticles are homogeneously dispersed in the surface. Disaggregation of ZnO NPs and adsorption of CAF on the surface was noticed due to alter the typical environment of nanoparticles. The adsorption of negatively CAF onto ZnO NPs makes the surface negatively charged result in repulsion between nanoparticles leading to dispersion of already aggregate nanoparticles.

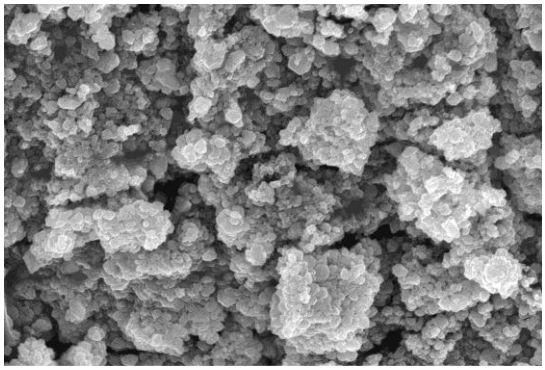

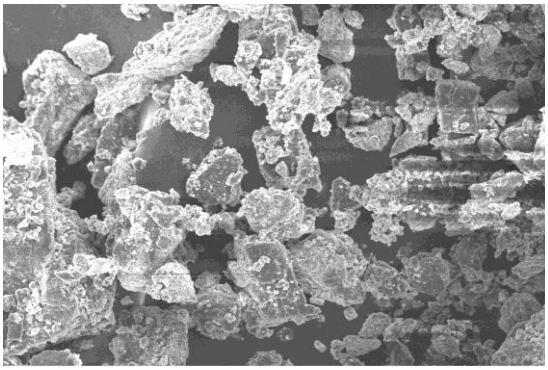

a) Unmodified ZnO NP Modified ZnO NP

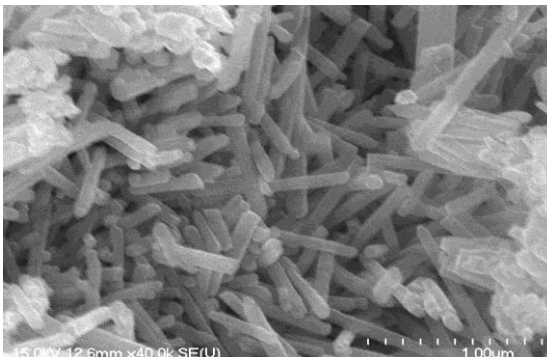

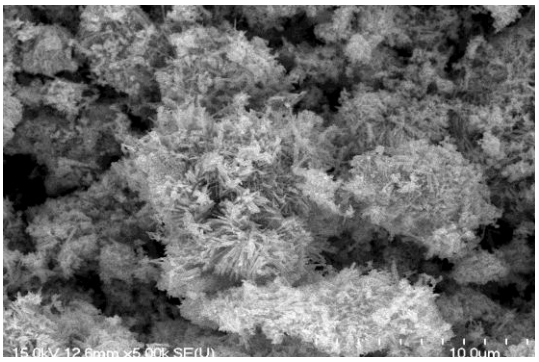

b) Unmodified ZnO NPs Modified ZnO NPs

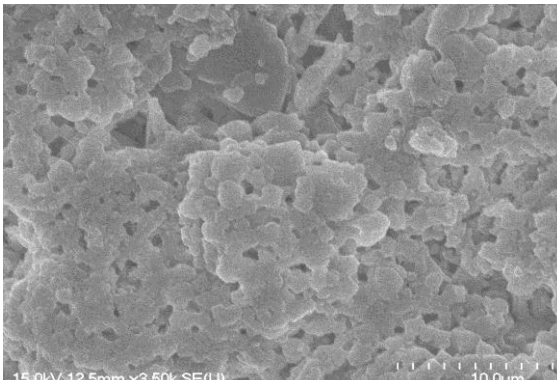

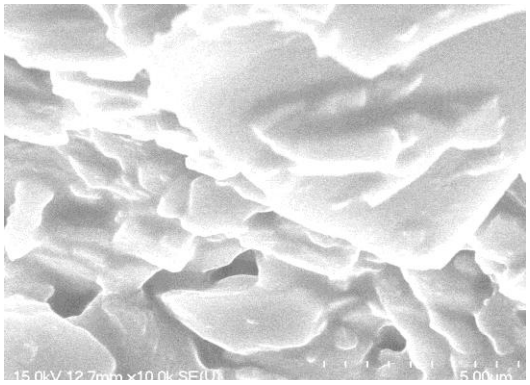

c) Unmodified ZnO NPs Modified ZnO NPs

Figure 4.2 : SEM micrographs of unmodified and modified ZnO NPs synthesised from a) zinc nitrate hexahydrate, b) zinc acetate dihydrate and c) zinc chloride

4.3 The UV-Vis absorption peak of ZnO nanoparticles

Figure 4.3 a-c shows the UV-Vis absorption pattern of unmodified ZnO nanoparticles dispersed in DMSO synthesised from $Zn(NO3)_2.6H_2O$,$Zn(CH3COO)_2.2H_2O$ and $ZnCl_2$ respectively. The absorption peak of ZnO nanoparticles was observed at 278 nm, 374nm and 378 nm for ZnCl2, $Zn(NO3)_2.6H_2O$ and $Zn(CH3COO)_2.2H_2O$ respectively. These peaks are due to electronic transition from deep level of valence band to conduction band. The UV-Vis absorption peak variation among the ZnO nanoparticles are due to the difference in their size and shape, which results due to a variety of precursors and calcination temperature [27, 28].

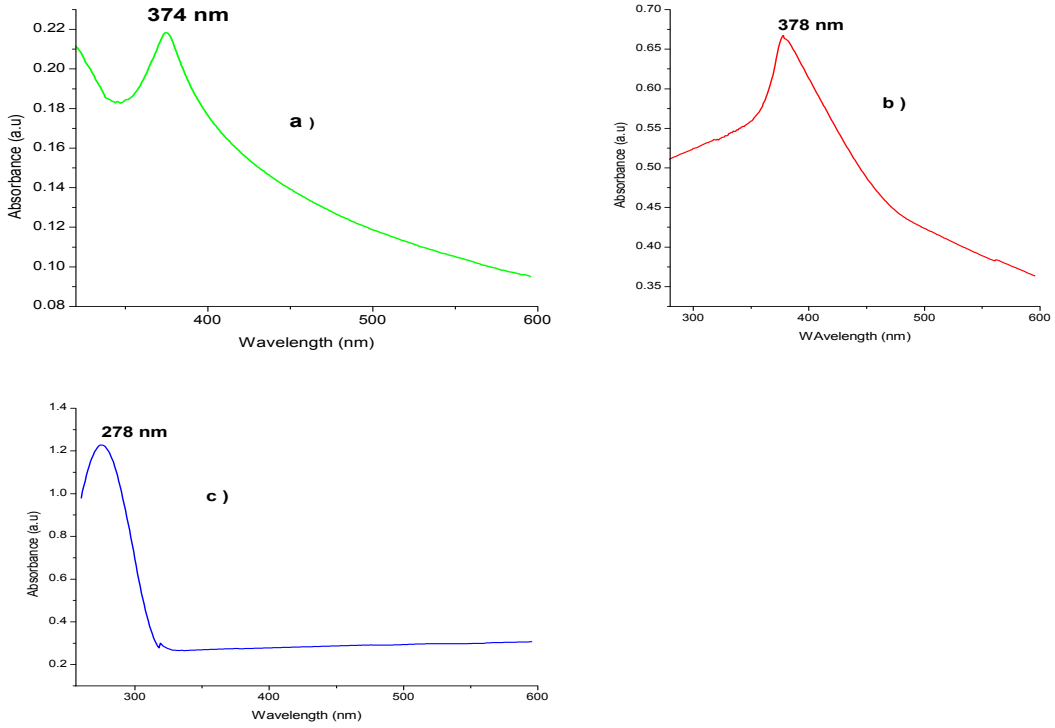

Figure 4.3 : UV-Vis absorption pattern of unmodified ZnO nanoparticles in DMSO synthesised using a) zinc nitrate hexahydrate, b) zinc acetate dihydrate and c) zinc chloride

4.4 IR spectra of ZnO nanoparticles

Figure 4.4 a-c shows the IR spectra of unmodified ZnO nanoparticles synthesised from $Zn(NO_3)_2.6H_2O$, $ZnCl_2$ and $Zn(CH3COO)_2.2H_2O$ respectively. The broad band observed in the wavenumber region 3437- 3466 cm^{-1} was due to O-H stretching, which represents the presence of water molecule on the surface of ZnO nanoparticles. Similarly, the band observed between 1370-1598 cm^{-1} were due to C=O stretching, which attached to the ZnO nanoparticles during synthesis. The sharp peak observed in the range 433 cm^{-1}- 510 cm^{-1} was attributed to the vibrational phonon of ZnO. This result indicates the successful production of ZnO nanoparticles [32].

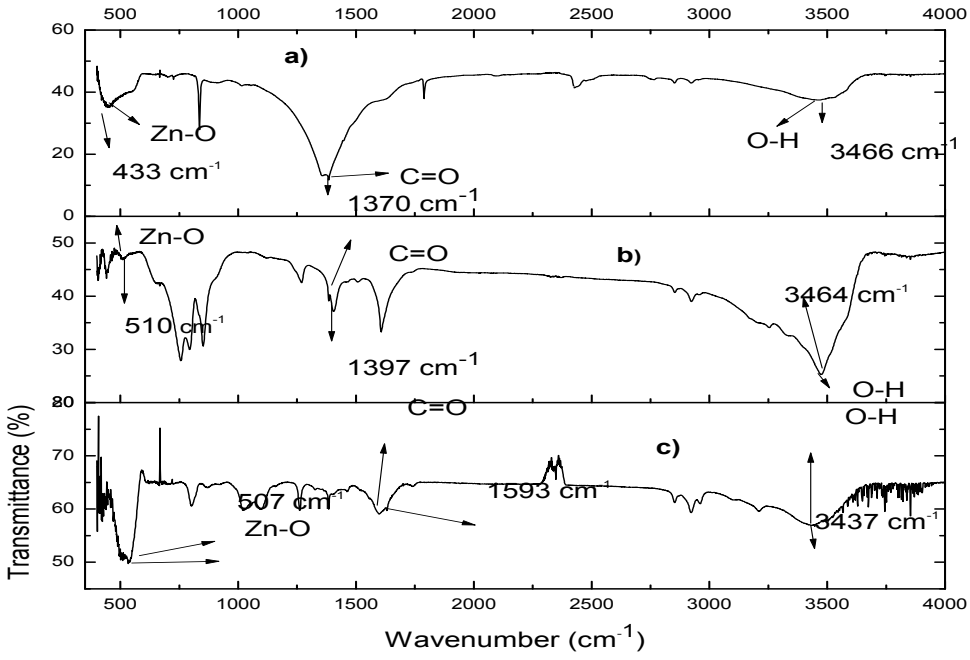

Figure 4.4: IR spectra of unmodified ZnO nanoparticles synthesised using a) zinc nitrate hexahydrate, b) zinc chloride and c) zinc acetate dihydrate

4.5 Emission spectra of ZnO nanoparticles

Figure 4.5 a-c shows the emission spectra of unmodified ZnO nanoparticles in DMSO synthesised using $Zn(CH3COO)_2.2H_2O$, $ZnCl_2$ and $Zn(NO3)_2.6H_2O$ respectively. The UV emission spectra peak of ZnO NPs synthesised from precursors $Zn(CH3COO)_2.2H_2O$, $ZnCl_2$ and $Zn(NO3)_2.6H_2O$ observed at 392 nm, 325 nm and 435 nm respectively are due to transition of free electrons from conduction band edge to valence band. On the other hand, the visible emission spectra were peaked at 455 nm, 466 nm and 469 nm for precursors $ZnCl_2$, $Zn(CH3COO)_2.2H_2O$ and $Zn(NO3)_2.6H_2O$ respectively. The cause of these visible emission spectra are the transition of electron from deep donor level to valence band due to oxygen vacancies and the transition from conduction band to deep acceptor level due to impurities and defect states [34] .

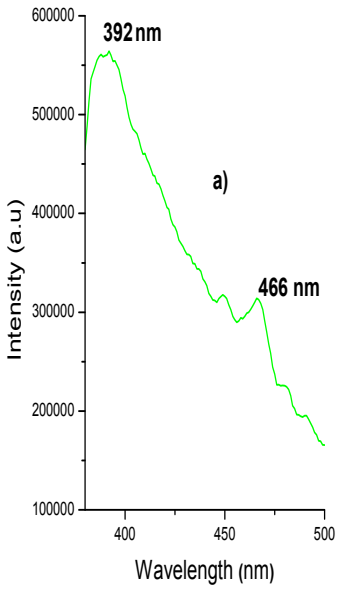

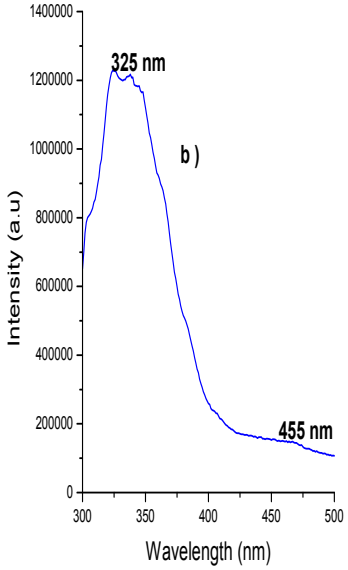

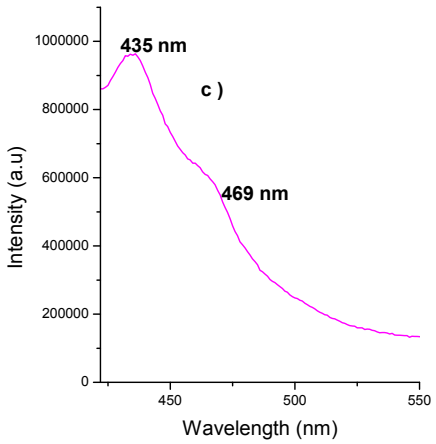

Figure 4.5: Emission spectra of unmodified ZnO nanoparticles in DMSO synthesised using a) zinc acetate dihydrate, b) zinc chloride and c) zinc nitrate hexahydrate

4.6 Antibacterial activity of the ZnO nanoparticles

Figure 4.6 a-c shows the antibacterial activity of ZnO nanoparticles synthesised from $ZnCl_2$, $Zn(NO3)_2.6H_2O$ and $Zn(CH3COO)_2.2H_2O$ on *E.coli* and *S. aureus* bacteria respectively. Antibacterial activity results shown that the ZnO nanoparticle synthesised using $ZnCl_2$ has been excellent antibacterial activity against both *S.aureus* and *E.coli* bacteria compared to the precursor $Zn(NO3)_2.6H_2O$ and $Zn(CH3COO)_2.2H_2O$. However, all the three ZnO nanoparticles showed admirable antibacterial activity than the standard antibiotic drug on *S.aureus* bacteria (Table 4.2). This is due to the simple cell wall membrane of *S.aureus.* As shown in the Table 4.2 a-c, the growth inhibition of *E.coli* and *S.aureus* has been increased by increasing the concentration of ZnO nanoparticles in discs. Generally, the result was indicated that ZnO NPs are more effective against Gram-positive bacterial strains (*S.aureus*) compared to Gram-negative bacterial strains (*E.coli*). The zone of inhibition produced by

unmodified ZnO NPs synthesised using $ZnCl_2$, $Zn(NO3)_2.6H_2O$ and $Zn(CH3COO)_2.2H_2O$ against *S.aureus* and *E.coli* is given in Table 4.2 a-c respectively.

a)

E.coli *S.aureus*

b)

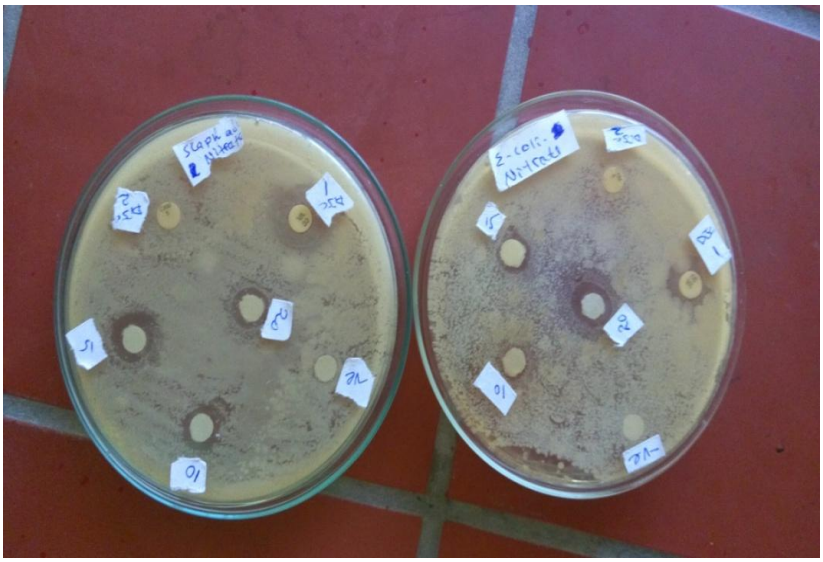

S.aureus *E.coli*

c)

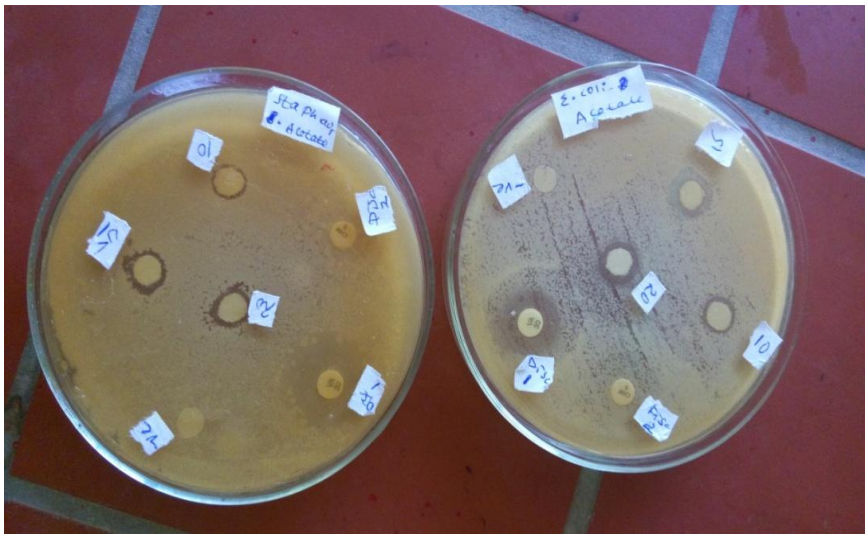

S.aureus *E.coli*

Figure 4.6: The antibacterial activity of unmodified ZnO NPs synthesised using a) zinc chloride, b) zinc nitrate hexahydrate and c) zinc acetate dihydrate on *S.aureus* and *E.coli*

Table 4.2: Zone of inhibition (ZOI) of unmodified ZnO NPs synthesised using a) zinc chloride, b) zinc nitrate hexahydrate and c) zinc acetate dihydrate on *E.*coli and *S. aureus*

a)

ZnO concentration in discs(mg/ml)	ZOI(mm)	
	E.coli	*S.aureus*
10	2	9
15	4	17
20	13	20
Standard drug(vancomycin)	10	11
Negative control	0	0

b)

ZnO concentration in discs(mg/ml)	ZOI(mm)	
	E.coli	*S.aureus*
10	6	11
15	10	12
20	12	13
Standard drug(vancomycin)	10	11
Negative control	0	0

c)

ZnO concentration in discs(mg/ml)	ZOI(mm)	
	E.coli	*S.aureus*
10	8	9
15	10	11
20	11	12
Standard drug(vancomycin)	10	11
Negative control	0	0

5 Conclusions

Zinc oxide nanoparticles have been synthesised using zinc acetate dihydrate, zinc chloride and zinc nitrate hexahydrate as a precursor via a wet chemical method. The synthesised ZnO nanoparticles were characterised by X-ray diffraction (XRD), Scanning Electron Microscopy (SEM), UV-Vis Spectroscopy, Fluorescence Spectroscopy and FTIR Spectroscopy. The averaged crystallite size of unmodified ZnO nanoparticles synthesised using zinc nitrate hexahydrate and zinc acetate dihydrate was about 28.09 nm and 31.86 nm respectively. The use of different salt precursors and calcination temperature leads to change in the particle size and shape of nanoparticles. The variation in UV-Vis absorption peaks of ZnO NPs indicates that the optical property of ZnO NPs is highly influenced by their shape and size. The vibrational phonon of ZnO observed in the range of 433 cm^{-1}- 510 cm^{-1} confirms the successful production of ZnO NPs. The ZnO nanoparticles showed two emission bands, an ultraviolet (UV) emission band due to the electronic transition from conduction band edge to valence band, and visible emission band due to defects that are related to deep level emissions. The adsorption of negatively charged caffeine on to ZnO NPs leads to dispersion of already aggregated nanoparticles. The synthesised ZnO NPs were also applied for antibacterial applications. All the three ZnO NPs have been shown admirable antibacterial activity than the standard antibiotic drugs on *S.aureus*. However, the ZnO NP synthesised using a precursor $ZnCl_2$ was revealed excellent antibacterial activity than the two precursors against both *S.aureus* and *E.coli*. Generally, the result in this study indicates that ZnO nanoparticles are more effective against *S.aureus* compared to *E.coli*.

References

[1] Sahoo, S. (2010): Socio-ethical issues and nanotechnology development: perspectives from India. IEEE Conference on Nanotechnology (IEEE-NANO), 1205–1210.

[2] Yadav, V. (2013): Nanotechnology, big things from a tiny world: areview. AEEE, 3(6): 771–778.

[3] Tomar, R.S., Shrivastava, V. and Chauhan, P.S. (2015): Nanobiotechnology: A potential tool for biomedics. World Journal of Pharmacy and Pharmaceutical Sciences, 4 (5): 1929-1943.

[4] Murty, B.S., Shankar, P., Raj, B., Rath, B.B. and Murday, J. (2013): Text book of nanoscience and nanotechnology, Berlin, Germany.

[5] Wyckoff, R.W.G. (1964): Crystal Structures, 2nd ed; Wiley: New York.

[6] Rai, M., Yadav, A. and Gade, A. (2009): Silver nanoparticles as a new generation of antimicrobials. Biotechnology Advances, 27(1): 76–83.

[7] Awodugba, A.O. and Ilyas, A.M.O. (2013): Synthesis and characterization of ZnO nanoparticles with zinc chloride as zinc source. Asian Journal of Natural and Applied Sciences, 2(2):41- 44.

[8] Ellmer, E. K., Klein, A. and Rech, B. (2008): Transparent conductive zinc oxide. Springer, Berlin, Germany.

[9] Anderson, J. and Chris, G.V.W. (2009): Fundamentals of zinc oxide as a semiconductor. Reports on Progress in Physics, 72: 1-29.

[10] Jayanta, K. B. (2012): Synthesis and characterization of ZnO nanoparticles. A thesis, National Institute of Technology, Rourkela, India.

[11] Segets, D., Gradl, J., Taylor, R.K., Vassilev, V. and Peukert, W. (2009): Analysis of optical absorbance spectra for the determination of ZnO nanoparticle size distribution, solubility, and surface energy. ACS Nano, 3(7): 1703–1710.

[12] Ling-min, Y., Xin-hui, F., lei, C., Jing-yi, S. and Wen, Y. (2012): Shape-controlled cluster growth of ZnO nanoflowers using sol–gel method. Micro and Nano Letters, 7: 1046-1048.

[13] Darroudia, M., Sabouric, Z., Oskueeb, R.K., Zake, A.K., Kargarc, H. and Hamid, M.H.N.A. (2013): Sol–gel synthesis, characterization and neuro toxicity effect of zinc oxide nanoparticles using gum tragacanth. Ceramics International, 24: 345-349.

[14] Singh, D.K., Pandey, D.K., Yadav, R.R. and Singh, D. (2012): A Study of nanosized zinc oxide and its nanofluid. Pramana Journal of Physics, 78(5):759-766.

[15] George, K.C., Soosen, S.M. and Lekshmi, B. (2009): Optical properties of ZnO nanoparticles. SB Academic Review, 16(1-2): 57-65.

[16] Gunasekaran, S., Shi, L. and Zhou, J. (2008): Low temperature fabrication of ZnO-whey protein isolate nanocomposite. Materials Letters, 62(28): 4383–4385.

[17] Jalal, R., Abareshi, M., Goharshadi, E.K., Moosavi, M., Yousefi, A. and Nancarrow, P. (2010): ZnO nanofluids: green synthesis, characterization and antibacterial activity. Materials Chemistry and Physics, 121(1–2): 198–201.

[18] Premanathan, M., Karthikeyan, K., Jeyasubramanian, K.and Manivannan, G. (2011): Selective toxicity of ZnO nanoparticles toward Gram-positive bacteria and cancer cells by apoptosis through lipid peroxidation. Nanomedicine: Nanotechnology, Biology and Medicine, 7(2): 184–192.

[19] Basha, S.K., Lakshmi, K.V. and Kumari, V.S. (2016): Ammonia sensor and antibacterial activities of green zinc oxide nanoparticles. Sensing and Bio-Sensing Research 10: 34-40.

[20] Qu, F. and Morais, P.C. (2001): The pH dependence of the surface charge density in oxide-based semiconductor nanoparticles immersed in aqueous solution. IEEE Transactions on Magnetic, 37: 2654–2656.

[21] Jagadish, C. and Pearton, S. (2012): Basic properties and applications of ZnO. The Australian national University, Canberra, ACT 0200, Australia.

[22] Meyer, B. K., Alves, H., Hofmann, D. M., Kriegseis, W., Forster, D., Bertram, F., Christen, J. Hoffmann, A., Straßburg, M., Dworzak, M., Haboeck, U. and Rodina A. V. (2004): Bound exciton and donor–acceptor pair recombinations in ZnO. Phys. Status Solidi B, 241(2): 231-260.

[23] Surya, P. G. (2012): Synthesis and characterization of zinc oxide nanoparticles by sol-gel methods. A thesis, National Institute of Technology, Rourkela, India.

[24] Paula, E., Jane, R.C., Renato, S.C. and Eber, A.A.M. (2012): Zinc oxide nanoparticles: Synthesis, antimicrobial activity and food packaging applications. Food and Bioprocess Technology, 5:1447–1464.

[25] Bonnell, D. (2001): Scanning probe microscopy and spectroscopy (1st edn). Wiley, New York.

[26] Burgess, C., Knowles, A., Chapman E. and Hall (1984): Practical absorption spectrometry, techniques in visible and ultraviolet spectrometry. 3: London.

[27] Banwell, C.N. and McCash, E.M. (1999): Fundamentals of molecular spectroscopy (4th edn.), McGraw- Hill International, UK.

[28] Imran, K. (2013): Structural and optical properties of Zr doped ZnO nano particles. Optmater., 35: 1189-1193.

[29] Sibilia, P. (1998): A guide to materials characterization and chemical analysis. VCH, New York.

[30] Nakamoto, K. (2009): Infrared and Raman spectra of inorganic and coordination compounds part A: Theory and Applications Inorganic Chemistry (6th edn.), Wiley Inter science, New York.

[31] Suhandro, P.P. and Rosari, S. (2012): Synthesis and spectroscopic characterization of undoped nanocrystalline ZnO nanoparticles prepared by co-precipitation. Journal of Material Science and Applications, 3: 530-537.

[32] West, A.R. (2003): Solid state chemistry and its applications. John Wiley &Sons, Singapore, Indian.

[33] Kommu, N. (2014): Applications of fluorescence spectroscopy. International Journal of Chemical and Pharmaceutical Sciences, 5: 18-21.

[34] Irimpan, L., Nampoori, V.P.N, Radhakrishnan, P., Deepthy, A. and Krishnan, B. (2007): Size dependent fluorescence spectroscopy of nanocolloids of ZnO. Journal of Applied Physics, 102 (1): 1-7.

[35] Amir, M.P. (2016): The synthesis, surface modification and use of metal-oxide nanoparticles in polyethylene for ultra-low transmission-loss HVDC cable insulation materials. Trita-Che Report, Stockholm 100 44, Sweden.

[36] Sawai, J., Shoji, S., Igarash, H., Hashimoto, A., Kokugan, T., Shimizu, M. and Kojima, H. (1998): Hydrogen peroxide as an antibacterial factor in zinc oxide powder slurry. Journal of Fermentation and Bioengineering, 86(5): 521–522.

[37] Gordon, T., Perlstein, B., Houbara, O., Felner, I., Banin, E. and Margel, S. (2011): Synthesis and characterization of zinc/iron oxide composite nanoparticles and their antibacterial properties. Colloids and Surfaces A: Physicochemical and Engineering Aspects, 374(1–3): 1–8.

[38] Applerot, G., Perkas, N., Amirian, G., Girshevitz, O. and Gedanken, A. (2009): Coating of glass with ZnO via ultrasonic irradiation and a study of its antibacterial properties. Applied Surface Science, 256(3): 53–58.

[39] Epand, R. M. and Epand, R. F. (2009): Lipid domains in bacterial membranes and the action of antimicrobial agents. Biochimica etBiophysica Acta (BBA)—Biomembranes, 1788(1): 289–294.

[40] Jones, N., Ray, B., Ranjit, K. T. and Manna, A. C. (2008): Antibacterial activity of ZnO nanoparticle suspensions on a broad spectrum of microorganisms. FEMS Microbiology Letters, 279(1): 71–76.

[41] Zhang, L., Ding, Y., Povey, M. and York, D. (2008): ZnO nanofluids—a potential antibacterial agent. Progress in Natural Science, 18(8): 939–944.

[42] Seven, O., Dindar, B., Aydemir, S., Metin, D., Ozinel, M. A. and Icli, S. (2004): Solar photocatalytic disinfection of a group of bacteria and fungi aqueous suspensions with TiO2, ZnO and Sahara Desert dust. Journal of Photochemistry and Photobiology A: Chemistry, 165(1–3): 103–107.

[43] Bradley, E.L., Castle, L. and Chaudhry, Q. (2011): Applications of nanomaterials in food packaging with a consideration of opportunities for developing countries. Trends in Food Science and Technology Press.

[44] Mayekar, J., Dhar, V. and Radha, S. (2014): Role of salt precursor in the synthesis of zinc oxide nanoparticles. International Journal of Research in Engineering and Technology, 3(3): 43- 45.

[45] Sawai, J. (2003): Quantitative evaluation of antibacterial activities of metallic oxide powders (ZnO, MgO and CaO) by conductimetric assay. Journal of Microbiological Methods, 54(2):177–182.

Declaration

I hereby declare that this M.sc thesis is my original work and has not been presented for a degree in any other universities, and that all sources of material used for the thesis have been properly acknowledged.

Name: Segedie Getie

Signature: .....

This M.sc thesis has been submitted to for examination with my approval as university advisor.

Name: Dr. Abebe Belay (Associate professor)

Signature: .....

Place and date of submission:

Applied Physics Program

Adama Science and Technology University

June, 2017